Kinetics of Electron Transfer and Oxygen Evolution in the Reaction of $[Ru(bpy)_3]^{3+}$ with Colloidal Iridium Oxide

Natalie D. Morris, Masahiro Suzuki,† and Thomas E. Mallouk*

Department of Chemistry, The Pennsylvania State University, University Park, Pennsylvania 16802

Received: May 9, 2004; In Final Form: August 13, 2004

The kinetics of electron transfer and oxygen evolution at citrate-stabilized $IrO_x{\cdot}nH_2O$ colloids were studied by time-resolved UV−visible spectrosopy and by steady-state photolysis of $[Ru(bpy)_3]^{2+}$ (bpy = 2,2′-bipyridyl) and persulfate in a hexafluorosilicate/bicarbonate buffer. Time-resolved studies of the reaction of $[Ru(bpy)_3]^{3+}$ with these colloids show an initial fast electron transfer, corresponding to oxidation of Ir(III) to Ir(IV). Further oxidation of surface Ir atoms occurs concomitantly with oxygen evolution with a second-order rate constant of $1.3 \times 10^6\ M^{-1}\ s^{-1}$. Both the time-resolved reduction of $[Ru(bpy)_3]^{3+}$ by $IrO_x{\cdot}nH_2O$ and the photocatalytic oxygen evolution under non-light-limited photolysis conditions have a H/D kinetic isotope effect (KIE) of 1.0. This contrasts with significantly higher KIE values for oxygen evolution from molecular *cis*,*cis*-$[(bpy)_2Ru(OH_2)]_2O]^{4+}$ and $[(terpy)(H_2O)Mn^{III}(O)_2(OH_2)terpy)]^{3+}$ water oxidation catalysts. This is consistent with the conclusion that, under the conditions of most photocatalytic experiments ($\sim 10^{-4}$ M $[Ru(bpy)_3]^{2+}$ concentration), electron transfer from the colloid to the oxidized sensitizer rather than formation of a surface-bound hydroperoxy species is the rate-determining step in photocatalytic oxygen evolution.

Introduction

The photochemical cleavage of water to generate hydrogen and oxygen has been studied since the early 1970s[1] and today remains one of the major challenges in the field of chemistry.[2] Overall water splitting has been demonstrated in series and tandem photoelectrochemical cells. However, these cells are either inefficient (because they employ polycrystalline photoelectrodes)[3] or very expensive (because they involve the use of complex single-crystal heterostructures).[4] Particles of wide-band-gap oxide semiconductors such as $SrTiO_3$ and $KTaO_3$ modified with Ni/NiO are inexpensive and perform the water splitting reaction reasonably well (quantum efficiency >20%), but they can do so only by using ultraviolet (UV) light.[5−10] Although cation and anion doping of oxide semiconductors has recently been shown to give photoactivity in the visible region,[11−14] the quantum yields of overall water splitting remain quite low (<1%).

An alternative approach to using a single material as a photocatalyst is to construct an integrated chemical system in which molecular sensitizers are coupled to semiconductor particles and molecular or colloidal hydrogen- and oxygen-evolving catalysts.[15] Dye sensitization has been used very successfully by Grätzel and co-workers in the design of regenerative photoelectrochemical cells[16] and has also been studied extensively in particle-based systems.[17] These systems are modular and are thus amenable to optimization of the individual components. We have recently studied dye-sensitized particle systems as photocatalysts for the hydrogen-[18] and oxygen-evolving[19] half reactions, but have not yet succeeded in coupling them for overall water splitting. A major problem in most systems of this type is the kinetic competition between back electron transfer reactions (which typically occur on a submillisecond time scale) and the thermal catalytic reactions that generate the chemical products, hydrogen and oxygen. Although the reduction of water to hydrogen at noble metal catalysts is facile, the water oxidation reaction is typically much slower.

In previous work,[20−22] we have studied and optimized the colloidal iridium oxide catalysts originally investigated by Harriman and co-workers[23−25] for the water oxidation half-reaction. Steady-state photolysis experiments established that, at high light intensity using optimized concentrations of sensitizer and colloid, the turnover rate of surface Ir atoms in $IrO_x{\cdot}nH_2O$ colloids was approximately $0.3\ s^{-1}$.[21] This is 3 orders of magnitude slower than back electron transfer in the best nonsacrificial, dye-sensitized hydrogen evolution systems.[18] An important question to ask is whether the oxygen evolution rate is limited by factors that can be altered by redesigning the system. For example, if the slow step is electron transfer between the oxidized sensitizer ($[Ru(bpy)_3]^{3+}$ (bpy = 2,2′-bipyridyl), or a polymer containing $[Ru(bpy)_3]^{3+}$ units[19]) and the colloidal catalyst, then the strategy would be to improve electronic coupling between them or to alter the ligands to increase the driving force for the electron-transfer reaction. If the slow step is O−O bond formation or M−O bond breaking on the colloid surface, however, then it would be more appropriate to redesign the colloidal catalyst itself.

We report here time-resolved experiments that show that a slow electron transfer between $[Ru(bpy)_3]^{3+}$ and $IrO_x{\cdot}nH_2O$ colloids occurs on the same time scale as oxygen evolution. We find a negligible H/D kinetic isotope effect (KIE ≈ 1.0) for both processes. Because a KIE significantly greater than 1.0 has been observed for molecular μ-oxo-bridged Ru and Mn complexes,[26−28] our data suggest that the rate-determining step deduced for those systems (formation of a metal-bound hydroperoxy group) is unlikely to be the slow step in oxygen evolution from $[Ru(bpy)_3]^{3+}$ and $IrO_x{\cdot}nH_2O$. The rate appears to be controlled by electron transfer between $[Ru(bpy)_3]^{3+}$ and surface Ir(IV) centers, which follows second-order kinetics. At high and

* To whom correspondence should be addressed. E-mail: tom@chem.psu.edu. Fax: 814-863-8403.

† Current address: Graduate School of Science and Technology, Shinshu University, Ueda, Nagano 386-8567, Japan.

10.1021/jp0480145 CCC: $27.50
Published on Web 09/28/2004

low concentrations of $[Ru(bpy)_3]^{3+}$ and $IrO_x{\cdot}nH_2O$, respectively, turnover rates per surface Ir atom as high as 160 s^{-1} (corresponding to 40 O_2 molecules per second) were measured.

Experimental Section

Materials. The $IrO_x{\cdot}nH_2O$ colloidal suspensions were prepared as described previously, except that dialysis was used instead of ion exchange to remove excess citrate ions.[20] $[Ru(bpy)_3]Cl_2{\cdot}6H_2O$ and potassium hexachloroiridate, K_2IrCl_6, were used as received from Aldrich and Alfa, respectively. Deionized water was passed through a Barnstead NanoPure II system to achieve a resistivity of 18.3 MΩ cm and was used to prepare all solutions.

Oxygen Evolution Reactions. Reaction conditions were the same as those reported previously, except that D_2O was used instead of H_2O in some experiments.[20] The concentrations of $[Ru(bpy)_3]^{2+}$, $IrO_x{\cdot}nH_2O$, Na_2SiF_6 from buffer, Na_2SO_4, and $Na_2S_2O_8$ were $(1.1-1.2) \times 10^{-4}$, 6.2×10^{-5}, 2.18×10^{-2}, 0.05, and 0.01 M, respectively. The buffer was made from 3.75×10^{-2} M Na_2SiF_6 by adding enough $NaHCO_3$ to make the pH 5.7. The concentration of $NaHCO_3$ in the buffer solution was approximately 8.0×10^{-2} M. The buffer solution was sonicated for 15 min, aged overnight, and then filtered. The reagents were sealed in a cell with a path length of 1.0 or 0.5 cm and purged with argon. The solution was then irradiated with light from a 450-W Xe/Hg lamp filtered using a 420-nm cutoff filter. One-milliliter headspace gas samples were analyzed for oxygen content by gas chromatography (GC) throughout the course of the reaction using a thermal conductivity detector and room-temperature molecular sieve 5A columns (Supelco).

Electron-Transfer Reactions. Electron-transfer reaction rates were measured as a function of $[Ru(bpy)_3]^{2+}$ and $IrO_x{\cdot}nH_2O$ concentration. All concentrations were held at the values listed above for steady-state photolysis, except that the concentration of $[Ru(bpy)_3]^{2+}$ was varied between 1.5×10^{-5} and 1.8×10^{-4} M and the final concentration of $IrO_x{\cdot}nH_2O$ was varied between 4.6×10^{-6} and 6.9×10^{-5} M. In each experiment, all reagents except $IrO_2{\cdot}xH_2O$ were added to a quartz cuvette equipped with a stir bar. The cuvette was irradiated for 20−30 s using a 450-W Xe/Hg lamp filtered by a 420-nm-cutoff filter to convert all of the $[Ru(bpy)_3]^{2+}$ to its oxidized form. After the appropriate amount of colloidal catalyst had been injected, the absorbance at 452 nm was monitored by using a HP 8452A diode array UV−vis spectrometer, with readings acquired every 0.1 s. Each set of conditions was analyzed three times, and the reported values are an average of the three runs.

Results and Discussion

Rate of Oxygen Evolution in Steady-State Photolysis. To establish the non-light-limited rate of water oxidation under steady-state photolysis conditions, $[Ru(bpy)_3]^{2+}/S_2O_8^{2-}$ solutions containing 6.2×10^{-5} M $IrO_x{\cdot}nH_2O$ were photolyzed in cells with path lengths of 1.0 and 0.5 cm. In the 1.0-cm cell, 1.0 mL of solution was irradiated using light from a Xe/Hg lamp with a 420-nm-cutoff filter. In the second experiment, 0.5 mL of the same solution was reacted in a 0.5-cm-path-length cell. The solution in the 1.0-cm-path-length cell absorbs 97% of the light at 452 nm, and the same solution in the 0.5-cm-path-length cell absorbs 83% of the light, based on the molar absorptivity of $[Ru(bpy)_3]^{2+}$ (14000 M^{-1} cm^{-1}) and its concentration (1.1×10^{-4} M). The initial oxygen evolution rates in the 1.0- and 0.5-cm cells were 0.23 and 0.13 μmol/min, respectively. The 1.0- and 0.5-cm cells contained 6.2×10^{-8} and 3.1×10^{-8} mol of Ir, respectively, and because the colloidal particles are 10−20 nm in diameter, approximately 15% of the atoms are on the surface. This corresponds to turnover rates, per surface Ir atom, of 0.41 and 0.45 O_2 molecule/s in the 1.0- and 0.5-cm cells, respectively. Because the amounts of light absorbed in the two cells were similar and the rate of oxygen evolution was proportional to the amount of catalyst present, it follows that the rate was not light-limited. The value obtained is roughly the same as the turnover rate (0.32 O_2 molecule/s per surface Ir atom) found previously by varying the light intensity in longer-path-length cells under similar conditions.[21]

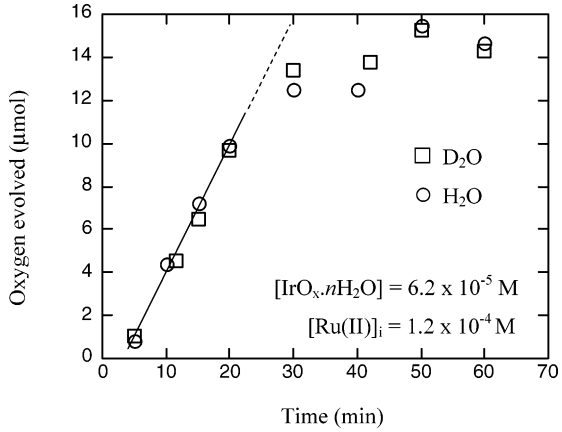

Figure 1. Oxygen evolution from 2.0 mL D_2O and H_2O persulfate/buffer solutions containing 1.1×10^{-4} M $[Ru(bpy)_3]^{2+}$ and 6.2×10^{-5} M $IrO_x{\cdot}nH_2O$ in a 1-cm-path-length cell.

If the oxygen evolution reaction rate is not light-limited (i.e., the rate is proportional to the amount of colloidal catalyst present), then there are several possibilities for the rate-determining step that should be distinguishable kinetically. The rate could be limited by bond rearrangements at the colloid surface or by other processes that occur within the colloidal particle, such as charge-transfer diffusion between Ir atoms. In this case, the reaction should be zeroth order in $[Ru(bpy)_3]^{3+}$. On the other hand, the reaction should be first order in $[Ru(bpy)_3]^{3+}$ if the rate-determining step is electron transfer between surface Ir atoms and $[Ru(bpy)_3]^{3+}$. This question is explored in more detail below by means of time-resolved experiments.

Figure 1 compares steady-state photolysis results obtained using H_2O and D_2O under non-light-limited conditions. Early in the reaction, the rate of oxygen evolution is constant at 0.49 μmol/min (0.44 molecule of O_2/s per surface Ir atom), but it falls progressively as the sensitizer is degraded.[20] Interestingly, the initial rate of oxygen evolution is the same in H_2O as in D_2O. This result contrasts with H/D kinetic isotope effects (KIEs) measured for molecular oxygen evolution catalysts. Hurst and co-workers attributed a KIE of 1.4 for the oxidation of water by *cis,cis*-$[(bpy)_2Ru(OH_2)]_2O]^{4+}$ to a rate-determining step involving the formation of a metal−hydroperoxy species. Limburg et al. found a KIE of 1.6−1.7 for catalytic oxygen evolution from solutions of HSO_5^- and $[(terpy)(H_2O)Mn^{III}(O)_2(OH_2)terpy)]^{3+}$, which is thought to involve a Mn(V) intermediate. If chemically similar Ir(V)−OOH species are involved in the oxidation of water by $IrO_x{\cdot}nH_2O$, their formation is apparently not rate-limiting under the conditions of our continuous photolysis experiments.

Time-Resolved Measurements of Electron-Transfer Rates. Because the generation of one molecule of oxygen corresponds to reduction of four $[Ru(bpy)_3]^{3+}$ ions,[29] the initial oxygen evolution rate of 0.49 μmol/min in the continuous photolysis experiment shown in Figure 1 corresponds to the reduction of

SCHEME 1: Preparation of $[Ru(bpy)_3]^{3+}$ Solutions[a]

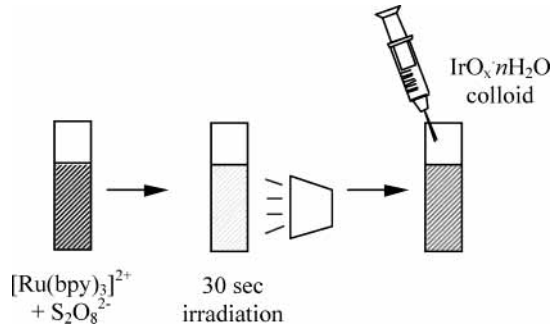

[a] $[Ru(bpy)_3]^{3+}$ solutions were prepared by 20−30-s irradiation of $[Ru(bpy)_3]^{2+}$/persulfate/buffer solutions, followed by rapid injection of $IrO_x{\cdot}nH_2O$ colloid to allow monitoring of electron-transfer kinetics on the 0.1−1.0-s timescale

$[Ru(bpy)_3]^{3+}$ ions at a rate of 3.3×10^{-8} mol/s, or 1.6×10^{-5} M/s in a 2.0 mL of solution. This rate can be compared to the rate of electron transfer between colloidal $IrO_x{\cdot}nH_2O$ and $[Ru(bpy)_3]^{3+}$ measured directly by the spectrophotometric method sketched in Scheme 1. By irradiating a bicarbonate-buffered (pH 5.7) solution containing persulfate for 20−30 s, $[Ru(bpy)_3]^{2+}$ is quantitatively oxidized to $[Ru(bpy)_3]^{3+}$. Under these conditions, the decomposition of $[Ru(bpy)_3]^{3+}$ occurs slowly (on a time scale of tens of minutes). Injection of the $IrO_x{\cdot}nH_2O$ colloid causes rapid reduction, which can be monitored by the reappearance of the $[Ru(bpy)_3]^{2+}$ absorbance at 452 nm.

Figure 2a shows plots of absorbance vs time, where $t = 0$ is defined as time of injection of the colloid. At all $[Ru(bpy)_3]^{2+}$concentrations shown in Figure 2a [$(2.2-18.3) \times 10^{-5}$ M, i.e., at Ru/Ir mole ratios of 0.5−4.0], the absorbance increases rapidly over the course of about 0.5 s and then reaches a plateau value corresponding to the complete conversion of $[Ru(bpy)_3]^{3+}$ to $[Ru(bpy)_3]^{2+}$. In a 1-cm-path-length cell, the concentrations of $[Ru(bpy)_3]^{3+}$ and $[Ru(bpy)_3]^{2+}$ ([Ru(III)] and [Ru(II)], respectively) can be calculated from the initial $[Ru(bpy)_3]^{2+}$ concentration ($[Ru(II)]_i$), the absorbance (A_{452}), and the extinction coefficients ($\epsilon_{Ru(III)}$ and $\epsilon_{Ru(II)} = 2300$ and 14000 M^{-1} cm^{-1}, respectively) as follows

$$A_{452} = \epsilon_{Ru(III)}[Ru(III)] + \epsilon_{Ru(II)}[Ru(II)] \quad (1)$$

$$[Ru(II)] = [Ru(II)]_i - [Ru(III)] \quad (2)$$

$$A_{452} = \epsilon_{Ru(III)}[Ru(III)] + \epsilon_{Ru(II)}([Ru(II)]_i - [Ru(III)]) \quad (3)$$

$$[Ru(III)] = \frac{\epsilon_{Ru(II)}[Ru(II)]_i - A_{452}}{\epsilon_{Ru(II)} - \epsilon_{Ru(III)}} \quad (4)$$

From eq 4, the absorbance vs time data can be converted to pseudo-first-order plots of ln[Ru(III)] vs time as shown in Figure 2b. These plots are approximately linear between 0 and 0.4 s. At higher values of the initial Ru(II) concentration, it is apparent that all of the lines have the same slope, whereas at lower values, the absolute value of the slope (and hence the pseudo-first-order rate constant) is larger.

Harriman et al. have found that citrate-stabilized $IrO_x{\cdot}nH_2O$ colloids, as prepared, contain equal amounts of Ir(III) and Ir(IV).[30] In solutions containing 4.6×10^{-5} M $IrO_x{\cdot}nH_2O$, the stoichiometric oxidation of Ir(III) to Ir(IV) should occur at an initial Ru(II) concentration of 2.3×10^{-5} M, i.e., at half the concentration of $IrO_x{\cdot}nH_2O$. Figure 3a shows a plot of the

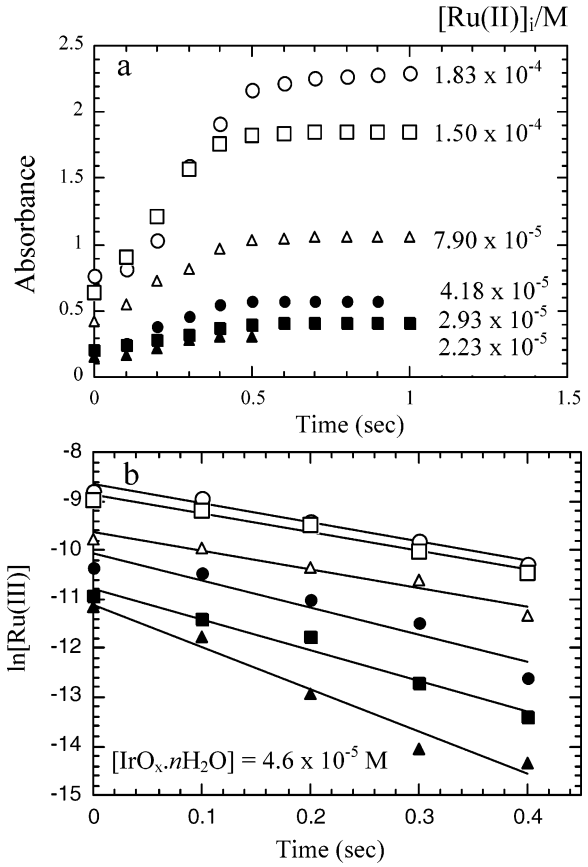

Figure 2. (a) Absorbance at 452 nm vs time for $[Ru(bpy)_3]^{3+}$ solutions prepared at different values of $[Ru(II)]_i$. The final concentration of $IrO_x{\cdot}nH_2O$ was 4.6×10^{-5} M. (b) Plots of ln[Ru(III)] vs time derived from the data in (a).

pseudo-first-order rate constant vs $[Ru(II)]_i$, obtained from the slopes of the lines in Figure 2b. At values of $[Ru(II)]_i$ below about 3×10^{-5} M, the reduction of $[Ru(bpy)_3]^{3+}$ by the colloid is relatively fast, with pseudo-first-order rate constants (k_{obs}) on the order of 10 s^{-1}. However, as $[Ru(II)]_i$ increases, the rate constant reaches a plateau of approximately 4 s^{-1}.

At the highest initial Ru(II) concentrations, there should be sufficient $[Ru(bpy)_3]^{3+}$ to oxidize the colloid well beyond the Ir(V) state. Therefore, it is reasonable to conclude that the plateau rate constant in Figure 3a corresponds to the catalytic oxidation of water by the $IrO_x{\cdot}nH_2O$ colloid. Interestingly, the same k_{obs} values are obtained, within experimental error, in H_2O and D_2O solutions. This is consistent with the data shown in Figure 1; that is, the KIE is near 1.0 at all values of $[Ru(II)]_i$. The fact that k_{obs} is invariant with $[Ru(II)]_i$ at high concentration means that, in the oxygen evolution regime, the reaction is first order in [Ru(III)], i.e.

$$\text{rate} = k_{obs}[Ru(III)] \approx k_{obs}[Ru(II)]_i \quad (5)$$

As noted above, this rate law is consistent with electron transfer between $[Ru(bpy)_3]^{3+}$ and surface Ir atoms (probably in the IV oxidation state) as the rate-determining step in the reaction.

Nahor et al. studied the oxidation of low-nuclearity $IrO_{1.6}{\cdot}nH_2O$ clusters by radiolytically generated OH radicals,[31] and they observed a similar stepwise oxidation process leading to water oxidation. Their predominantly Ir(III) clusters (initial average oxidation state of 3.2) were first oxidized to a mixed Ir(III)−Ir(IV) form (average oxidation state of 3.8) in a first-order process with a rate constant of 320 s^{-1}. A second oxidation, which was thought to involve the formation of an

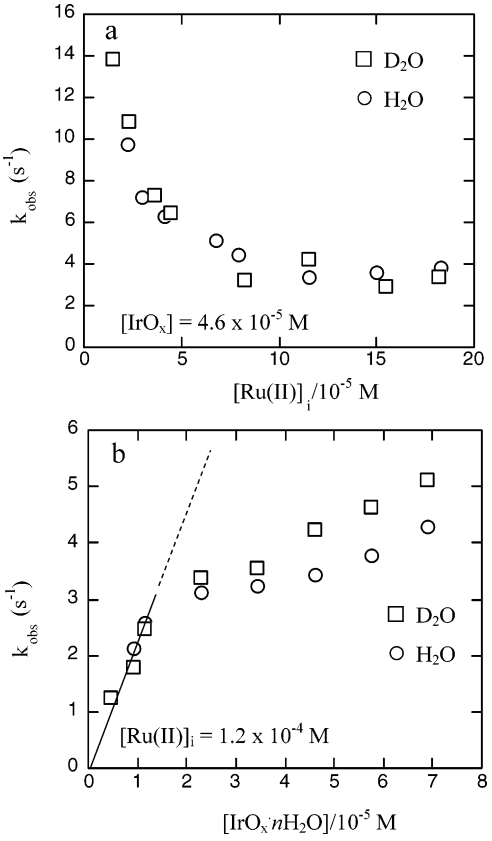

Figure 3. (a) Pseudo-first-order rate constant (k_{obs}) vs $[Ru(II)]_i$ for electron-transfer measurements in H_2O and D_2O, at a final $IrO_x{\cdot}nH_2O$ concentration of 4.6×10^{-5} M. (b) k_{obs} vs $[IrO_x{\cdot}nH_2O]$ at $[Ru(II)]_i = 1.2 \times 10^{-4}$ M in H_2O and D_2O.

unstable Ir(V) intermediate, occurred concomitantly with oxygen evolution with a first-order rate constant of 7 s^{-1}. Both oxidation processes were accompanied by the release of protons from the clusters, which is consistent with the rapid changes in solution conductivity observed by Grätzel and co-workers in flash photolysis of colloidal TiO_2/RuO_2 solutions containing $[Ru(bpy)_3]^{2+}$ and persulfate.[32] The $IrO_x{\cdot}nH_2O$ colloids used in our experiments are much larger (10−20 nm in diameter) than those studied by Nahor et al.,[31] meaning that approximately 15% of the Ir atoms are on the surface. However, the oxidation states involved in water oxidation and the time scale of the stepwise oxidations appear similar.

Figure 3b shows the effect of varying the concentration of $IrO_x{\cdot}nH_2O$ injected into 1.2×10^{-4} M $[Ru(bpy)_3]^{3+}$ solutions. In the oxygen evolution regime, at high ratios of $Ru(II)_i/IrO_x{\cdot}nH_2O$ where k_{obs} is independent of $[Ru(II)]_i$, there is a linear relationship between the pseudo-first-order rate constant and the $IrO_x{\cdot}nH_2O$ concentration. From the slope of the line (2.0×10^5 M^{-1} s^{-1}) and the fraction of atoms on the surface of the colloid (0.15), we can derive a second-order rate constant k_2 of 1.3×10^6 M^{-1} s^{-1}.

$$k_{obs} = k_2[IrO_x{\cdot}nH_2O]_{surf} \quad (6)$$

Under these conditions, the turnover rate of surface Ir atoms is $k_2[Ru(III)]$, about 160 s^{-1}, which corresponds to O_2 evolution at a rate of about 40 molecules/s per surface Ir atom.

Conclusions

Electron transfer from colloidal $IrO_x{\cdot}nH_2O$ to $[Ru(bpy)_3]^{3+}$ proceeds in a stepwise fashion, and oxidation of the colloid beyond the Ir(IV) state leads to oxygen evolution. At the concentration of $[Ru(bpy)_3]^{2+}$ ($\sim 10^{-4}$ M) typically used in steady-state photolysis experiments, the rate-determining step in the process is electron transfer between $[Ru(bpy)_3]^{3+}$ and surface Ir(IV), which occurs with a second-order rate constant of 1.3×10^6 M^{-1} s^{-1}. This slow electron-transfer reaction—and the fact that the steady-state concentration of $[Ru(bpy)_3]^{3+}$ is a small fraction of the total sensitizer concentration in most photolysis experiments—leads to the low turnover rates typically observed. At high $[Ru(bpy)_3]^{3+}$ concentrations, turnover rates as high as 160 s^{-1} (corresponding to 40 O_2 molecules s^{-1}) per surface Ir atom were observed in time-resolved measurements. The H/D KIE of 1.0 found under these conditions is consistent with electron transfer as the rate-determining step, and it follows that the catalyst-limited turnover rate must be greater than 40 O_2 molecules per second per surface Ir atom. This suggests that it might be possible to design more efficient systems for photochemical oxygen evolution, and possibly nonsacrificial systems for overall water splitting, by using high local concentrations of sensitizer molecules (e.g., by directly coupling the sensitizer to the colloid) or by increasing the driving force for electron transfer between the oxidized sensitizer and the colloidal catalyst.

Acknowledgment. We thank Prof. James Hurst for providing preprints of his papers on the mechanism of oxygen evolution by μ-oxo-bridged Ru complexes. This work was supported by the Division of Chemical Sciences, Office of Basic Energy Sciences, U.S. Department of Energy, under Contract DE-FG02-93ER14374.

References and Notes

(1) Fujishima, A.; Honda, K. *Nature* **1972**, *238*, 37.
(2) Bard, A. J.; Fox, M. A. *Acc. Chem. Res.* **1995**, *28*, 141.
(3) Smotkin, E. S.; Cervera-March, S.; Bard, A. J.; Campion, A.; Fox, M. A.; Mallouk, T. E.; Webber, S. E.; White, J. M. *J. Phys. Chem.* **1987**, *91*, 6.
(4) Khaselev, O.; Turner, J. A. *Science* **1998**, *280*, 425.
(5) Takata, T.; Tanaka, A.; Hara, M.; Kondo, J. N.; Domen, K. *Catal. Today* **1998**, *44*, 17.
(6) Yoshimura, J.; Ebina, Y.; Kondo, J.; Domen, K.; Tanaka, A. *J. Phys. Chem.* **1993**, *97*, 1970.
(7) Tokunaga, S.; Kato, H.; Kudo, A. *Chem. Mater.* **2001**, *13*, 4624.
(8) Kato, H.; Kudo, A. *J. Phys. Chem. B* **2001**, *105*, 4285.
(9) Kudo, A.; Kato, H. *Chem. Phys. Lett.* **2000**, *331*, 373.
(10) Kudo, A.; Mikami, I. *Chem. Lett.* **1998**, 1027.
(11) Zou, Z.; Ye, J.; Sayama, K.; Arakawa, H. *Nature* **2001**, *414*, 625.
(12) Asahi, R.; Mirokawa, T.; Ohwaki, T.; Aoki, K.; Taga, Y. *Science* **2001**, *293*, 269.
(13) Kasahara, A.; Nukumizu, K.; Takata, T.; Kondo, J. N.; Hara, M.; Kobayashi, H.; Domen, K. *J. Phys. Chem. B* **2003**, *107*, 791.
(14) Kasahara, A.; Nukumizu, K.; Hitoki, G.; Takata, T.; Kondo, J. N.; Hara, M.; Kobayashi, H.; Domen, K. *J. Phys. Chem. A* **2002**, *106*, 6750.
(15) Bard, A. J. *Integrated Chemical Systems*; John Wiley and Sons: New York, 1994; pp 227−288.
(16) Grätzel, M. *Nature* **2001**, *414*, 338.
(17) Kamat, P. V. *Chem. Rev.* **1993**, *93*, 267.
(18) Saupe, G. B.; Mallouk, T. E.; Kim, W.; Schmehl, R. H. *J. Phys Chem. B* **1997**, *101*, 2508.
(19) Hara, M.; Lean, J. T.; Mallouk, T. E. *Chem. Mater.* **2001**, *13*, 4668.
(20) Hara, M.; Waraksa, C. C.; Lean, J. T.; Lewis, B. A.; Mallouk, T. E. *J. Phys. Chem. A* **2000**, *104*, 5275.
(21) Hara, M.; Mallouk, T. E. *J. Chem. Soc., Chem. Commun.* **2000**, 1903.
(22) Morris, N. D.; Mallouk, T. E. *J. Am. Chem. Soc.* **2002**, *124*, 11114.
(23) Harriman, A.; Richoux, M.; Christensen, P. A.; Mosseri, S.; Neta, P. *J. Chem. Soc., Faraday Trans. 1* **1987**, *83*, 3001.
(24) Harriman, A.; Thomas, J. M.; Millward, G. R. *New J. Chem.* **1987**, *11*, 757.
(25) Harriman, A.; Pickering, I. J.; Thomas, J. M.; Christensen, P. A. *J. Chem. Soc., Faraday Trans. 1* **1988**, *84*, 2795.
(26) Yamada, H.; Siems, W. F.; Koike, T.; Hurst, J. K. *J. Am. Chem. Soc.***2004**, *126*, 9786 .

(27) Hurst, J. K. *Coord. Chem. Rev.*, in press.

(28) Limburg, J.; Vrettos, J. S.; Chen, H.; de Paula, J. C.; Crabtree, R. H.; Brudvig, G. W. *J. Am. Chem. Soc.* **2001**, *123*, 423.

(29) In the photocatalytic production of $[Ru(bpy)_3]^{3+}$ and/or oxygen from $[Ru(bpy)_3]^{2+}$/persulfate solutions, the production of one O_2 molecule involves the conversion of two photons, as reduction of $S_2O_8^{2-}$ by $[Ru(bpy)_3]^{2+*}$ generates the SO_4^{-} radical anion, which oxidizes a second $[Ru(bpy)_3]^{2+}$ ion to $[Ru(bpy)_3]^{3+}$. However, the generation of one O_2 molecule involves the reduction of four $[Ru(bpy)_3]^{3+}$ ions under all conditions.

(30) Harriman, A.; Nahor, G. S.; Mosseri, S.; Neta, P. *J. Chem. Soc., Faraday Trans. 1* **1988**, *84*, 2821.

(31) Nahor, G. S.; Hapiot, P.; Neta, P.; Harriman, A. *J. Phys. Chem.* **1991**, *95*, 616.

(32) Humphry-Baker, R.; Lilie, J.; Grätzel, M. *J. Am. Chem. Soc*. **1982**, *104*, 422.